J. Membrane Biol. 180, 147–161 (2001)
DOI: 10.1007/s002320010066

The Journal of
Membrane
Biology

Temperature-Dependent Expression of a Squid Kv1 Channel in Sf9 Cells and Functional Comparison with the Native Delayed Rectifier

M.W. Brock[1], **Z.N. Lebaric, H. Neumeister***, **A. DeTomaso****, **W.F. Gilly**
Hopkins Marine Station of Stanford University, Department of Biological Sciences, Pacific Grove, CA 93950, USA
[1]Neurosciences Program of Stanford University, Stanford, CA 94305, USA

Abstract. SqKv1A is a cDNA that encodes a Kv1 (*Shaker*-type) α-subunit expressed only in the giant axon and the parental giant fiber lobe (GFL) neurons of the squid stellate ganglion. We incorporated SqKv1A into a recombinant baculovirus for expression in the insect Sf9 cell line. Whole-cell patch-clamp recordings reveal that very few cells display functional potassium current (I_K) if cultured at the standard postinfection temperature of 27°C. At 18°C, less SqKv1A protein is produced than at 27°C, but cells with I_K currents are much more numerous and can survive for at least 20 days postinfection (vs. ~5 days at 27°C). Activation and deactivation kinetics of SqKv1A in Sf9 cells are slower (~3- and 10-fold, respectively) than those of native channels in GFL neurons, but have similar voltage dependencies. The two cell types show only subtle differences in steady-state voltage-dependence of conductance and inactivation. Rates of I_K inactivation in 20 mM external K are identical in the two cell types, but the sensitivity of inactivation to external tetraethylammonium (TEA) and K ions differ: inactivation of SqKv1A in Sf9 cells is slowed by external TEA and K ions, whereas inactivation of GFL I_K is largely insensitive. Functional differences are discussed in terms of factors that may be specific to cell-type, including the presence of presently unidentified Kv1 subunits in GFL neurons that might form heteromultimers with SqKv1A.

Key words: Potassium channel — Insect cells — Temperature — Activation — Inactivation — Pharmacology

* *Present address:* Department of Neuroscience, Albert Einstein College of Medicine, Bronx, NY 10461, USA

** *Present address:* Department of Immunology, Stanford University School of Medicine, Stanford, CA 94305, USA

Correspondence to: W.F. Gilly

Introduction

Voltage-gated potassium (Kv) channels confer diverse electrical properties on neurons and other types of excitable cells (Rudy, 1988), and products of numerous Kv α-subunit genes and splice-variants form K channels that differ widely in biophysical and pharmacological properties (Jan & Jan, 1997). Functional diversity is further extended through heteromultimer formation by α-subunits within a subfamily (Isacoff, Jan & Jan, 1990; McCormack et al., 1990; Ruppersberg et al., 1990; Sheng et al., 1993; Wang et al., 1993; Weiser et al., 1994; Blaine & Ribera, 1998), post-translational modifications of Kv α-subunits (Drain, Dubin & Aldrich, 1994; Levitan, 1994; Thornhill et al., 1996), and by association with Kvβ-subunits (reviewed in Xu & Li, 1998; Pongs et al., 1999). These mechanisms lead to a rich assortment of Kv phenotypes (Jan & Jan, 1990).

Comparison of native channels with their cloned counterparts in heterologous expression systems is fundamental in evaluating the biological relevance of phenomena identified through approaches like mutagenesis or co-expression. Although it is now routine to isolate Kv cDNAs and carry out heterologous expression studies, it remains problematic to analyze functional and biochemical properties of specific Kv gene products in native neurons and most other cell types. Such efforts are hampered by difficulty in isolating monotypic cells expressing the channel of interest, by potential mixtures of Kv gene-products in single cells, and by complex cellular geometry.

Potassium current (I_K) of the squid giant axon, responsible for the falling phase of the propagated action potential, is arguably the most extensively characterized native I_K. This has been facilitated by the system's unparalleled amenability to electrophysiological approaches and by its relatively simple complement of Kv channels. Macroscopic and single-channel recordings

from giant axons (Conti & Neher, 1980; Llano, Webb & Bezanilla, 1988) and cell bodies of the parental giant fiber lobe (GFL) neurons (Llano & Bookman, 1986) indicate the predominant contribution of one channel type to the classical 'delayed rectifier' I_K in *Loligo peleai* and *L. opalescens* (Perozo, Jong & Bezanilla, 1991; Perozo et al., 1991; Nealey et al., 1993; Mathes et al., 1997).

SqKv1A is a squid cDNA encoding a K channel α-subunit homologous to those encoded by the Drosophila *Shaker* gene and Kv1 genes in mammals. The proposal has been made that SqKv1A subunits form the delayed rectifier K channels in the squid giant axon system (Rosenthal, Vickery & Gilly, 1996). Arguments supporting this assignment include: (i) SqKv1A mRNA is found within the stellate ganglion only in the somata of the monotypic GFL neurons. (ii) Immunoblots reveal protein corresponding to SqKv1A α-subunits in both GFL somata and in the fused giant axons. (iii) When expressed in *Xenopus* oocytes, SqKv1A channels mediate an inactivating I_K that is similar to that of the native delayed rectifier at both macroscopic and single channel levels (*see also* Jerng & Gilly, 2000). (iv) SqKv1A and native channels are blocked by tityustoxin Kα, and in both cases this block depends strongly on pH (Dudlak, Jerng & Gilly, 2000). (v) Native channels and SqKv1A are sensitive to the Kv1-selective blocker, S-nitrosodithiothreitol (Brock, Mathes & Gilly, 1997; Brock & Gilly, 2000).

For many types of electrophysiological analysis, the oocyte expression system presents limitations. Analysis of rapid gating kinetics is problematic in the two-electrode configuration, and patches are often too short-lived for complex experimental protocols. A whole-cell recording environment is often desirable for these reasons. To this end, we have incorporated SqKv1A into a recombinant baculovirus for heterologous expression in Sf9 insect cells, which do not display any endogenous voltage-gated currents (Klaiber et al., 1990).

Functional expression of SqKv1A was virtually nonexistent at the standard Sf9 culture temperature of 27°C. However, a lower culture temperature (18°C) more characteristic of native expression in the squid was found to be permissive. Whole-cell patch-clamp recordings indicate that most functional properties of SqKv1A channels are similar to those of native channels and those of SqKv1A in oocytes. However, several significant differences in voltage-dependent gating parameters and pharmacological properties do exist between the cloned channels and their putative native counterparts. Some of these differences suggest the existence of important influences of presently unknown cellular factors on channel function. The possibility of heteromultimer formation between SqKv1A and a presently unidentified Kv1 subunit in GFL neurons is also raised.

Materials and Methods

Production of Recombinant Baculovirus

Recombinant baculovirus was constructed, isolated, and purified by standard procedures (Summers & Smith, 1987). Deletion of the codon for valine at position 5 of the SqKv1A coding sequence was carried out by PCR-based mutagenesis of a previously described SqKv1A-pBSTA construct (Rosenthal et al., 1996; Rosenthal, Liu & Gilly, 1997). Functional expression of SqKv1A ΔV5 mRNA in *Xenopus* oocytes is 5–10-fold higher than that of wild type SqKv1A, but channel functional properties in oocytes are indistinguishable (Liu, 1999; and *unpublished results*). The full coding sequence of this mutant, flanked by the 5′ and 3′ untranslated regions of the *Xenopus* β-globin gene (part of pBSTA), was subcloned into the baculovirus transfer vector pVL1392 (Stratagene, La Jolla, CA). Sf9 cells were cotransfected with this final construct and wild-type baculovirus (AcMNPV) DNA. Recombinant virus was isolated by plaque assay and purified by two rounds of plaque purification. Recombinant viral stocks were prepared from purified plaques, titered, and stored at 4°C. Recombinant baculovirus containing the N-terminal deletion mutant of *Drosophila Shaker*B cDNA (ShBΔ6-46; Hoshi, Zagotta & Aldrich, 1990) was a gift of Dr. Min Li, Johns Hopkins University, Baltimore, MD.

Maintenance and Infection of Sf9 Cells

Spodoptera frugiperda cells of the Sf9 line (ATCC, Rockville, MD) were maintained in suspension at 27°C in Grace's Insect Medium (Life Technologies, Gaithersburg, MD) supplemented with 3.3 mg/ml lactalbumin hydrolysate, 3.3 mg/ml yeastolate, 50 μg/ml streptomycin, 50 units/ml penicillin, 1.25 μg/ml fungizone, and 10% fetal bovine serum (Sigma, St. Louis, MO) according to standard protocols (Summers & Smith, 1987). For infections, log-phase cells were seeded in 35 mm culture dishes (for electrophysiology and immunoblots) or onto sterile 12 mm round glass coverslips in 24-well culture plates (for immunocytochemistry) at 1×10^6 cells/ml and allowed to attach for 30 to 60 min. The media was then removed and inoculum was added at a multiplicity of infection of 5–10. After 1 hr the inoculum was replaced with fresh medium. Infected cells were maintained at 18°C or 27°C as described below. For electrophysiological and immunoblot studies, fresh medium (0.5 ml) was added to each culture dish every three days. Assays were performed at the indicated time points.

Isolation and Maintenance of GFL Neurons

Adult squid (*Loligo opalescens*) were obtained from Monterey Bay, CA and housed in circular laboratory tanks plumbed with flow-through sea water for up to 1 week. GFL cell bodies were isolated from the posterior tip of the stellate ganglion and maintained in primary culture at 16°C as previously described (Gilly, Lucero & Horrigan, 1990). Cells were normally used for recording within two days of isolation.

Antibodies

Production and purification of polyclonal $Ab_{87\text{-}215}$, directed against a bacterial fusion protein containing amino acids 87-215 of SqKv1A, has been previously described (Rosenthal et al., 1996). $Ab_{1\text{-}15}$ was directed

against a synthetic peptide (Protein and Nucleic Acid Facility, Stanford University) corresponding to amino acids 1–15 of SqKv1A with an acetylated N-terminus. This peptide was conjugated via a C-terminal cysteine to keyhole limpet hemocyanin and used for antisera production in New Zealand white rabbits (Immuno-Dynamics, La Jolla, CA). Antibodies were affinity-purified using the peptide coupled to a thiopropyl-Sepharose 6B column (Pierce, Rockford, IL).

Immunoblotting

Crude Sf9 cell membranes were prepared as described by DeTomaso et al. (1993) with minor modifications. Lysis buffer contained 250 mM sucrose, 20 mM HEPES (pH 7.4), 1 mM EDTA , 1 mM PMSF, 10 μg/ml leupeptin, and 10 μg/ml aprotinin. Final spins were for 30 min at 50,000 × *g*. Protein concentration was determined using a standard BCA assay. Samples were subjected to SDS-PAGE electrophoresis (7.5% gels) and transferred to a PVDF membrane which was then incubated in phosphate-buffered saline (PBS: 137 mM NaCl, 2.7 mM KCl, 10 mM Na_2HPO_4, 1.8 mM KH_2PO_4, pH 7.2) containing 10% nonfat dry milk (pH 7.4). Both primary antisera were used at a dilution of 1:1000 in PBS. For blocking controls, undiluted antisera were incubated overnight at 4°C with their respective peptide antigen at a final concentration of 0.5 mg/ml. Goat anti-rabbit secondary antibodies conjugated to horseradish peroxidase (Sigma, St. Louis, MO) were used at a 1:5000 dilution. Detection employed enhanced chemiluminescence (Renaissance, NEN, Boston, MA).

Immunocytochemistry

Sf9 cells were processed following conventional procedures (DeTomaso et al., 1993). Primary antibodies ($Ab_{87\text{-}215}$ and $Ab_{1\text{-}15}$) were diluted 1:500. Goat anti-rabbit secondary antibodies conjugated to Texas Red (Molecular Probes, Eugene, OR) were used at a dilution of 1:1000. Upon completion of processing, the coverslip carrying the cells was inverted and placed onto a drop of anti-bleaching solution (Slowfade, Molecular Probes, Eugene, OR) on a glass slide for viewing and photography using an Olympus BH2 microscope with an RFCA fluorescence attachment and Kodak TMAX 400 film. Control experiments utilized noninfected Sf9 cells processed in the above manner and infected Sf9 cells incubated with secondary antibody only.

Electrophysiology

Recordings of I_K from Sf9 cells were obtained with an EPC7 amplifier (HEKA, Lambrecht/Pfalz, Germany) using standard whole-cell patch-clamp techniques. Recordings from GFL cells were obtained using an amplifier of conventional design with a 20 MΩ feedback resistor. Data sampling and pulse generation were controlled with software written by Dr. D.R. Matteson, University of Maryland, Baltimore, MD. Electrodes of 0.5–1.5 MΩ resistance were pulled from borosilicate glass (for Sf9 cells; VWR, So. Plainfield, NJ) or 7052 glass (for GFL cells; Garner, Claremont, CA), fire-polished, and coated with Sylgard (Dow Corning, Midland, MI) to reduce pipette capacitance. Holding potential was −80 mV throughout. Records were filtered at either 5.0–8.0 kHz for sampling at 20 kHz and down to 0.5 kHz for 2 kHz sampling. All recordings were made at 18°C.

Recording solutions for Sf9 and GFL cells were designed to have compositions as similar as possible. Unless otherwise indicated, Sf9 internal solution (pH 7.0) contained (in mM): 20 KCl, 50 KF, 80 K-glutamate, 3 lysine, 10 HEPES, 1 EGTA, 1 EDTA, 26 glycine, 85 sucrose, and 4 tetramethylammonium hydroxide. GFL internal solution was identical but contained an additional 355 mM glycine (381 mM total) and 206 mM sucrose (291 mM total); 4 mM MgATP was added from aliquots of 200 mM frozen stock to the internal solutions immediately before use (Mathes et al., 1997), and pH was readjusted using TMA-OH.

Sf9 external solution (pH 7.2) contained (in mM): 20 KCl, 168 NaCl, 10 $CaCl_2$, 10 $MgCl_2$, 10 $MgSO_4$, 5 HEPES, 1.6 NaOH. GFL external solution (pH 7.6) contained an additional 312 NaCl. A number of experiments with GFL neurons were also carried out in external solutions lacking this additional NaCl (osmolality maintained with sucrose), so that the ionic strength matched that of Sf9 solutions. This difference in ionic strength caused no marked differences in kinetic or steady state properties of I_K, and did not increase sensitivity of I_K inactivation to external K or TEA (*data not illustrated*). In experiments where external TEA or K concentrations were varied, these cations replaced Na on an equimolar basis. Solution changing was carried out with a flow-through system.

For electrophysiological recording a 10 μl volume of Sf9 cells was harvested from an infected master dish by gently withdrawing medium from the bottom of the dish using a sterile pipette tip. The cells were then transferred directly to a recording chamber containing external solution. In this manner, cells from the same infected dish could be studied on different days following infection. Peak outward I_K at +40 mV was used to assay the level of functional expression in individual cells. Whole-cell capacitance was estimated from the integral of the capacity current accompanying a −10 mV voltage step, and this value was used to derive peak I_K density at +40 mV (units of pA/pF). Series resistance was electronically compensated as much as possible, and the effective access resistance was estimated from the integral and time course of the capacity current (Armstrong & Gilly, 1992). Data from experiments with a calculated voltage error of more than 10 mV were discarded.

Sf9 Cell Viability Assay

A 1 μl volume of 4% trypan blue was added to 10 μl of Sf9 cells collected as described above, and the mixture was transferred onto a hemacytometer. Fractional viability was calculated as the number of nonstained cells divided by the total number of cells.

Results

Expression of SqKv1A in Sf9 Cells

Expression of SqKv1A α-subunit protein was assayed using two different polyclonal antisera directed against distinct domains of the predicted amino acid sequence. $Ab_{87\text{-}215}$ was directed against a portion of the SqKv1A protein that includes the well conserved T1 (Shen et al., 1993) or NAB (Yu, Xu & Li, 1996) domain of Kv1 α-subunits. $Ab_{1\text{-}15}$ was directed against the unique N-terminal sequence of SqKv1A.

Figure 1 shows immunoblots of crude membrane fractions prepared from Sf9 cells maintained at 27°C for 3 days postinfection (p.i.). In samples from SqKv1A-infected cells, both antibodies recognize a major band of 50–52 kD and at least one minor band closer to the 55.7 kD size predicted for the SqKv1A core-polypeptide (Fig. 1A and B, lane 1). Neither antibody recognizes protein from noninfected cells (lane 4), cells infected with wild-

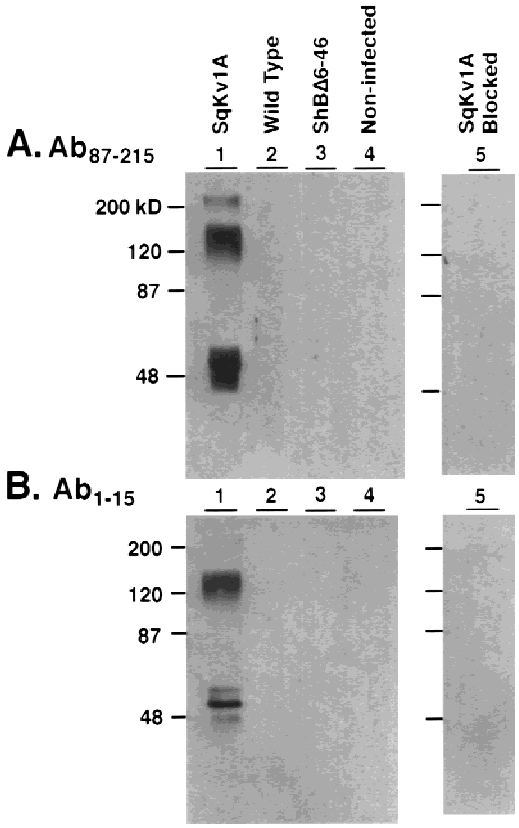

Fig. 1. Identification of SqKv1A protein in infected Sf9 cells with immunoblots using affinity-purified polyclonal antibodies $Ab_{87\text{-}215}$ (*A*) or $Ab_{1\text{-}15}$ (*B*). Cells were processed 3 days after infection with SqKv1A baculovirus (*Lanes 1*), wild-type AcMNPV virus (*Lanes 2*) or ShBΔ6-46 virus (*Lanes 3*). *Lanes 4* show results with noninfected cells. *Lanes 5* show results with antibodies that had been blocked by pre-absorption of the respective antigen (*see* Materials and Methods). Bands of the expected size for SqKv1A monomers (~50 kD) are present only in samples from SqKv1A-infected cells. Material of higher apparent molecular weight (>120 kD) presumably represents aggregated SqKv1A protein. All cells were maintained at 27°C p.i.

type baculovirus (lane 2) or cells infected with a virus encoding the *Drosophila* ShBΔ6-46 potassium channel. Specificity of both antisera for SqKv1A protein is further demonstrated by controls in which immunoreactivity with SqKv1A was blocked by pre-absorbing each antiserum with its respective antigen (lane 5).

Bands above 120 kD are also recognized by both antibodies. These bands are absent in all control experiments and presumably represent aggregation of SqKv1A protein. Similar results have been reported in work on *Shaker* channels (Klaiber et al., 1990; Santacruz-Toloza et al., 1994). Under our experimental conditions, disulfide bond formation should be minimal, but noncovalent association may still occur (Schulteis, Nagaya & Papazian, 1996).

Although SqKv1A protein is readily detected in cells incubated at a p.i. temperature of 27°C, which is standard for the Sf9 cell system, very few SqKv1A-infected cells incubated at this temperature express functional channels (*see below*). However, 18°C was found to be permissive for functional expression. Figure 2*Ai* illustrates a family of whole-cell I_K records obtained from a typical SqKv1A-infected cell incubated at 18°C (4 days p.i.). Selectivity for K ions was confirmed by testing the dependence of reversal potential on external K concentration (*data not shown*). These records are similar to cell-attached patch recordings from *Xenopus* oocytes injected with SqKv1A cRNA and from squid GFL neurons in which this gene is expressed (Rosenthal et al., 1996; *see also below*). Very little, if any, I_K with similar voltage- and time-dependent properties is present in a typical SqKv1A-infected cell incubated 4 days p.i. at 27°C (Fig. 2*Bi*). In a very small number of 27°C-incubated cells, however, small I_K can be detected, and a more detailed analysis of I_K levels at both p.i. temperatures is presented below.

Both infected and noninfected Sf9 cells sometimes show small, nonlinear outward leak currents at positive voltages, and this current is responsible for the initial jump at the beginning of the records in Fig. 2. I_K through SqKv1A channels can easily be distinguished from this leak by its sigmoidal activation time course and prominent tail currents. The leak current is obvious only in cells with low input resistance ($<1 \times 10^9$ ohm), but the relative contributions of seal *vs.* membrane nonlinearities is not clear. Noninfected cells, cells infected with wild-type baculovirus (*data not shown*), and most SqKv1A-infected cells incubated at 27°C (Fig. 2*Bi*) show only this leak current.

Immunocytochemical Localization of SqKv1A Protein

Although the presence of I_K in SqKv1A-infected cells incubated at 18°C indicates the existence of functional SqKv1A channels in the cell membrane at 4 days p.i., immunocytochemical examination of infected cells using $Ab_{87\text{-}215}$ indicates that most SqKv1A protein appears to be intracellular (Fig. 2*Aii*). Although the signal intensity varies from cell to cell, nearly every cell shows fluorescence far above the background level seen in noninfected cells processed in an identical manner (Fig. 2*Aiii*) or of SqKv1A-infected cells treated only with secondary antibody (Fig. 2*Aiv*). Experiments using $Ab_{1\text{-}15}$ yielded results similar to those described here at 1, 4 and 7 days p.i. (*not shown*).

Despite the poor expression of functional SqKv1A channels at 27°C, a large amount of SqKv1A protein is produced at this temperature. Figure 2*Bii* shows immunocytochemical results with cells that were incubated at 27°C but were otherwise treated, processed, and photographed identically to the 18°C-incubated cells. Label-

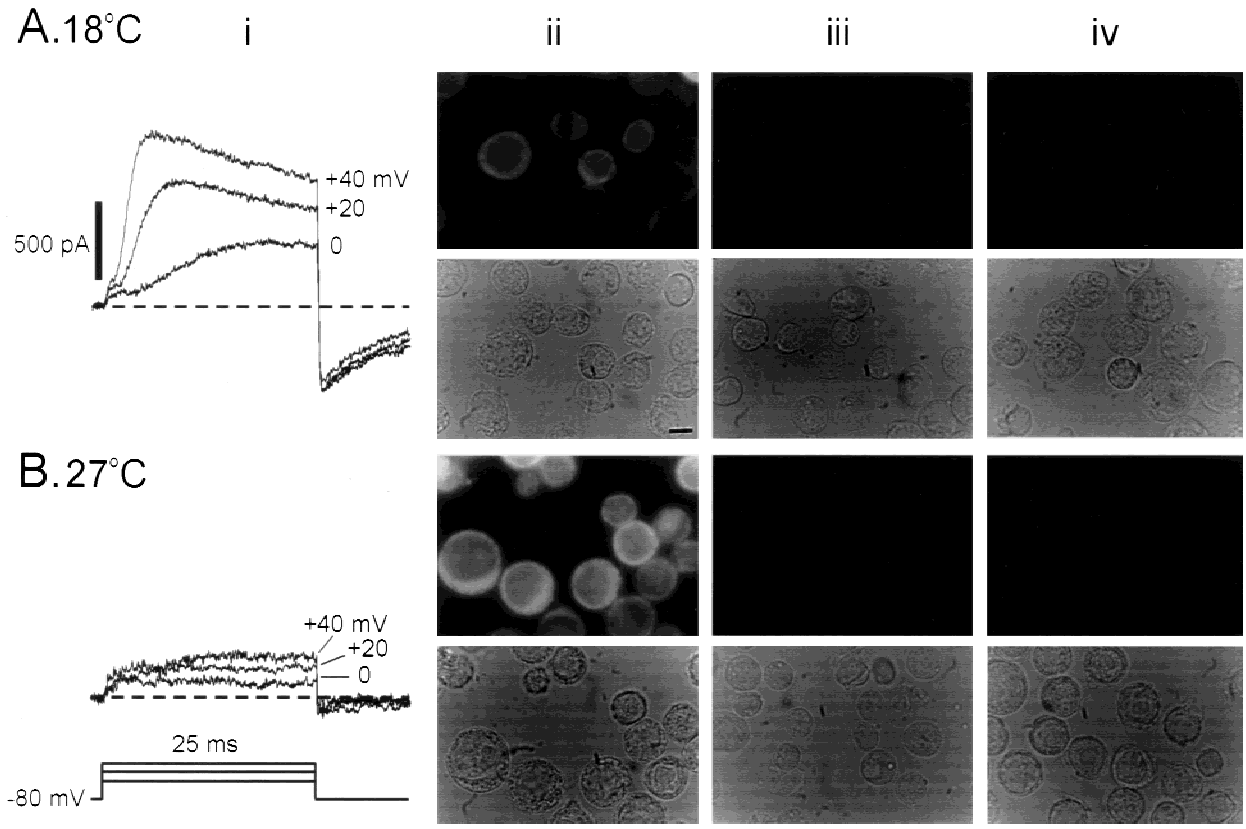

Fig. 2. Expression of SqKv1A in Sf9 cells at 18°C (*A*) and 27°C (*B*). Both parts of the figure are arranged in the following order: (i) Currents recorded using whole-cell patch-clamp at three different voltages are displayed. Voltage-dependent I_K due to functional SqKv1A channels are present at 18°C (*A*) but not at 27°C (*B*) where only small nonspecific leak currents are evident. This difference is typical. (ii) Immunocytochemical analysis of expression in SqKv1A-infected cells using $Ab_{87\text{-}215}$ and a Texas Red-labeled secondary antibody. Upper panel displays epi-fluorescence image; lower panel displays matching bright-field image. (iii) Control using same antibodies as in ii but with noninfected cells. (iv) Control using SqKv1A-infected cells exposed to secondary antibody only. All experiments were carried out 4 days p.i. The scale bar in the lower panel of *Aii* represents 10 μm and applies to all micrographs in this figure.

ing is visibly more intense in the 27°C-incubated cells and again appears to be predominately intracellular. No labeling is seen with noninfected cells (Fig. 2*Biii*) or infected cells treated with secondary antibody only (Fig. 2*Biv*).

Temperature-Dependent Expression of SqKv1A Protein *vs.* Functional Channels

Results above reveal a disparity between the total amount of SqKv1A protein produced in infected Sf9 cells and the level of functional channels attained. This phenomenon was explored further using immunoblots and whole-cell recordings.

Crude membrane fractions from cells infected with SqKv1A and then incubated at 27°C or 18°C were prepared each day for 5 days p.i., and immunoblots were performed with equal amounts of total cellular protein from these fractions. SqKv1A protein appears on day 1 p.i. at 27°C, and its level peaks around day 3 (Fig. 3*B*). At 18°C, SqKv1A protein is not detected until day 2, and the peak level is attained on days 3–4 (Fig. 3*A*). Although the time courses of protein expression are roughly similar, there is more SqKv1A protein at 27°C than at 18°C at all times.

These results contrast with those obtained for functional SqKv1A channels assayed by whole-cell recordings from cells of the same infections used for the immunoblot analyses. Peak outward I_K density (in pA/pF) for a voltage step to +40 mV was used as an indicator of the density of functional channels, and results from all cells studied are presented in Fig. 3*C*. I_K is first detectable on day 3 p.i. at each temperature. At 27°C, average I_K density is maximal on this day, although very small, and declines to an undetectable level by day 5. At 18°C, however, average I_K density rises dramatically between days 3 and 4, and remains high on day 5. Expression of functional channels with respect to the amount of α-subunit protein is thus far more efficient at 18°C than

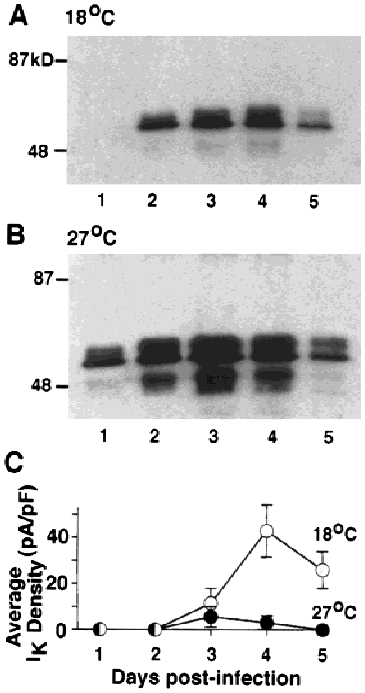

Fig. 3. Comparison of the time course of expression for total SqKv1A protein *vs.* functional channels at 18°C and 27°C. (*A*) Immunoblot analysis of total SqKv1A protein in crude membrane fractions from cells maintained at 18°C and processed on days 1–5 p.i. (*B*) Results of the same experiment as in *A* but carried out on cells maintained p.i. at 27°C. Total SqKv1A protein at 27°C is greater than that at 18°C at all days tested. (*C*) Functional SqKv1A channels were assayed by whole-cell voltage-clamp (peak I_K at +40 mV) using cells from the same infections as those providing material for *A* and *B*. Functional expression at 18°C is much more robust and peaks on day 4, with differences in average I_K density (calculated for all cells assayed, including those with no detectable I_K) between the two temperatures being significant on days 4 and 5 ($P < 0.05$).

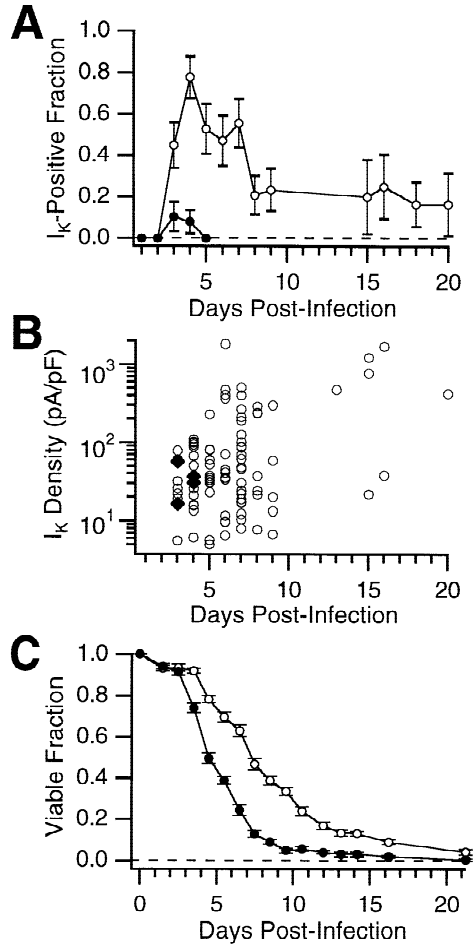

Fig. 4. Changes in functional expression of SqKv1A channels over longer times p.i. (*A*) The fraction of cells showing detectable I_K (*see* Results) depends strongly on temperature and changes over time. *Closed circles* are from cells maintained at 27°C p.i.; *open circles* are from cells at 18°C p.i. (Means ± SEM). (*B*) I_K density as determined in individual cells at early times (days 3 and 4) is comparable in cells maintained at 27°C (*closed diamonds*) and at 18°C (*open circles*). I_K in 18°C cells tends to increase over time, and cells expressing large I_K can be found after 2 weeks p.i. (*C*) The time course of the decline in viability of SqKv1A-infected cells (determined by trypan blue exclusion) depends on temperature. *Closed circles* are from cells at 27°C p.i.; *open circles* are from cells at 18°C p.i. (Means ± SEM).

at 27°C. This phenomenon does not reflect differences in the efficiency of infection, as a higher multiplicity of infection did not augment functional expression at either temperature (*data not shown*).

Even though immunofluorescence data indicate that virtually every infected cell expresses SqKv1A protein at either temperature, the fraction of cells displaying functional I_K depends strongly on temperature. Individual cells were studied at different times p.i. (up to 20 days) and were scored as being either positive (I_K+) or negative for I_K as described in conjunction with Fig. 2. Pooled results from several infections are summarized in Fig. 4*A*. The fraction of I_K+ cells is much higher at 18°C than at 27°C at all times after day 2, but I_K density in individual cells does not appear to depend on temperature on days 3 and 4 (Fig. 4*B*). These data indicate that the strong temperature-dependence for average I_K density described in conjunction with Fig. 3*C* is primarily due to the very small fraction of I_K+ cells at 27°C.

Figure 4*A* also illustrates that at 18°C, I_K+ cells can be found until at least day 20 p.i. At these later times, individual I_K densities (Fig. 4*B*) reach levels much higher than the averages for early time points displayed in Fig. 3*C*. Individual I_K densities at these later times (~1,000 pA/pF) are comparable to those of native GFL neurons (*unpublished data*).

A similar analysis with 27°C-incubated cells after day 5 p.i. was not possible, because the fragility of the cells prevented successful whole-cell recordings. This reflects a difference between temperatures in viral pathogenesis that was also evident from viability assays (Fig.

4*C*). Viability, as assayed with a standard trypan-blue test, remained high (>90%) for both 18°C- and 27°C-incubated cells through day 3, after which viability at 27°C fell precipitously. At 18°C, viability declined more slowly and remained higher than at 27°C for the duration of the experiment. This extension of cell-viability at 18°C was also observed for cells infected with the recombinant ShBΔ6-46 baculovirus (*data not shown*).

Functional Comparison of SqKv1A Channels in Sf9 Cells with Native Channels in GFL Neurons

Activation and Deactivation Properties

Sf9 cells provide an excellent whole-cell recording environment which allows a relatively straightforward comparison of SqKv1A I_K with the native delayed rectifier I_K in GFL neurons. Although the general appearance of I_K is quite similar in the two preparations (Fig. 5*A*), some significant differences exist.

Probably the most obvious difference concerns channel deactivation responsible for the tail currents following a depolarizing voltage step. Figure 5*B* shows I_K tails for both preparations following 5 msec depolarizations that produced no inactivation. Deactivation kinetics are well described by a single exponential decay (τ_{OFF}) at each voltage illustrated. Figure 5*C* establishes the voltage dependence of τ_{OFF} from a population analysis of Sf9 cells and GFL neurons. At every voltage τ_{OFF} is about 10-fold slower in the Sf9 cells, but the actual voltage-dependence of τ_{OFF} is comparable in both cases, changing e-fold in 54 mV.

I_K activation was analyzed using the method of Schoppa and Sigworth (1998*a*) in which the sigmoidal activation time course is approximated by a delay parameter (δ) and an exponential time constant (τ_{ON}; *see* inset in Fig. 5*C*). τ_{ON} is derived from a single exponential fit to the I_K waveform between 50–100% of peak amplitude. δ is calculated as the time between the onset of the activating depolarization and the extrapolated zero-current intercept of the aforementioned exponential fit. In an activation scheme involving multiple state transitions, τ_{ON} approximates the time constant of the rate-limiting transition at a given voltage, and δ describes a latency compounded by all other transitions.

Activation kinetics are also slower in Sf9 cells. Results in Fig. 5*C* indicate that the voltage-dependence of δ is nearly identical for Sf9 cells and GFL neurons, and that δ is about 2.5-fold slower at all voltages in Sf9 cells than in GFL neurons. δ values for both cell types fall into two distinct ranges of exponential voltage-dependence. A range of higher voltage-dependence exists between −10 to +20 mV (K_1), and a less voltage-dependent range lies between +30 and +60 mV (K_2). Similar 'breaks' in the voltage-dependence of δ have been observed for ShB (Schoppa & Sigworth, 1998*a*). Comparison of τ_{ON} is more complicated, because the overall τ_{ON}-*V* relationships become parallel only near the upper limit of the tested voltages, where Sf9 values are about 2-fold slower. Positive to this range, the same voltage-dependent transition is likely to be rate-limiting in both cases. The nonexponential shape of both curves at more negative voltages suggests that no single transition is rate-limiting, making interpretation difficult. A detailed model of activation for SqKv1A channels or for the native channels has yet to be developed.

A more subtle difference exists between the two preparations in the voltage-dependence of peak K conductance (g_K). g_K was measured as $\Delta I_K/\Delta V$ from depolarizing pulses that were terminated at the time of peak I_K (*see* inset in Fig. 6*A*), and the g_K-*V* relations for a representative SqKv1A-infected Sf9 cell and GFL neuron are plotted in Fig. 6*A*. In both preparations g_K reaches its 50% level at a similar voltage, but the overall g_K-*V* relation rises more steeply in the Sf9 cell. In order to compare g_K-*V* curves in the two cell types, we used fits to 4th-power Boltzmann relationships to derive parameters for slope and position on the voltage axis. We do not wish to imply that this equation accurately describes the mechanism of activation gating in the present case (Zagotta, Hoshi & Aldrich, 1994; Zagotta et al., 1994; Baker et al., 1998; Schoppa & Sigworth, 1998*a*,*b*), and use it only as a matter of convenience and convention. The solid curves in Fig. 6*A* are fits (*see* Fig. 6 legend) to the data sets with single-subunit midpoints ($V_{1/2}$) of −19.0 mV (Sf9) *vs.* −28.5 mV (GFL) and equivalent charges (*z*) of 2.82 e_0 (Sf9) *vs.* 1.77 e_0 (GFL). Similar results were obtained in four cells of each type (*see* Fig. 6 legend). The *z* value for Sf9 cells is significantly higher than that for GFL cells ($P < 0.01$ by Student's *t*-test). $V_{1/2}$ values for the two cell types are not significantly different.

Figure 6*B* directly compares the slope of the g_K-V relations for an Sf9 cell and a GFL neuron at voltages where conductance is relatively low. The Sf9 data are shifted along the voltage axis by −20 mV for comparison. At very negative voltages, the slopes are similar (~ e-fold change in 6 mV), but as described above, in Sf9 cells g_K rises more steeply between −40 mV and +20 mV than it does in GFL neurons.

Inactivation Properties

Long depolarizations produce substantial inactivation of I_K in both Sf9 cells and GFL neurons (Fig. 7*A*). Inactivation kinetics at positive voltages were characterized by fitting a single exponential (τ_{INAC}) to the decay of outward I_K during a depolarization of 250 msec. At +40 mV τ_{INAC} is 48 ± 6 msec (mean ± SEM) in Sf9 cells and 42 ± 3 msec in GFL neurons ($n = 5$ in both cases), and

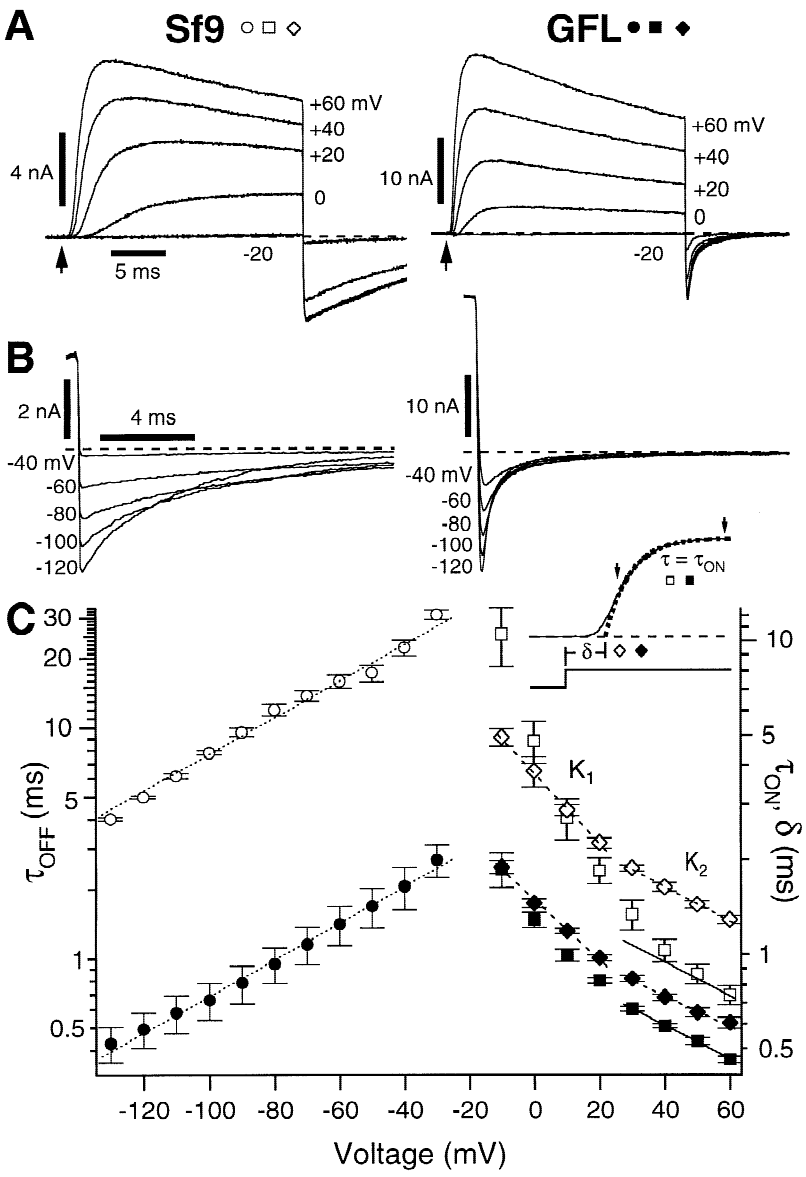

Fig. 5. I_K activation and deactivation kinetics recorded from Sf9 cells expressing SqKv1A and from GFL neurons. (*A*) I_K elicited with 25 msec depolarizations from −80 mV to the indicated voltages. (*B*) Deactivation tails at the indicated voltages following 5 msec depolarizations to +40 mV (Sf9) or +60 mV (GFL). (*C*) Voltage-dependence of I_K activation and deactivation kinetics for Sf9 (*open symbols*) and GFL (*closed symbols*) cells. Points represent mean ± SEM for 4 cells of each type. Note difference in range of right and left axes. Values of τ_{OFF} (*circles*) were obtained by fitting I_K tails at each voltage with a single exponential decay by the least-squares method (not illustrated). The hand-fitted *dotted lines* have identical logarithmic slopes of e-fold/54 mV. Activation parameters were derived by fitting the final 50% of activation (denoted with *arrowheads*) with the function,

$$I = I_{peak}\,(1 - e^{(\delta - t)/\tau_{ON}}),$$

where the delay parameter δ (*diamonds*) represents the extrapolated zero-current time-point of an exponential relaxation with time constant τ_{ON} (*squares*) and peak amplitude I_{peak} (*see inset* and Results). The τ_{ON}-V relationships for Sf9 cells and GFL neurons approach a similar slope at very positive voltages, and the hand-fitted *solid lines* have identical slopes of e-fold/−80.8mV. The value of δ has a similar voltage-dependence for Sf9 cells and GFL neurons, and falls into two distinct ranges of exponential voltage-dependence, denoted by K_1 and K_2. The slope of the hand-fitted *dashed lines* through the data points in the K_1 and K_2 ranges are e-fold/−38.9mV and e-fold/−79.1mV respectively for Sf9 cells, and e-fold/−45.5mV and e-fold/−88.7mV for GFL neurons.

there is very little voltage-dependence in this parameter in either preparation positive to +20 mV, where the g_K-V relation is essentially saturated (Fig. 7*B*). Differences between the values of τ_{INAC} for Sf9 cells and GFL neurons are insignificant at all illustrated voltages ($P > 0.05$ by Student's *t*-test).

Inactivation at negative voltages is more difficult to compare. Inactivation of native I_K in GFL neurons and giant axons is complex, exhibiting fast and slow kinetic components (Mathes et al., 1997). The relative importance of these components depends on both voltage and temperature, with more positive voltages (above 0 mV) and higher temperatures (above 12°C) favoring the fast fraction. Inactivation revealed in GFL neurons with the above test is thus predominately of the fast type. At negative voltages where few channels open, e.g. −40 mV, inactivation of native I_K is primarily slow (τ_{INAC} = 300 msec; Mathes et al., 1997). At the intermediate voltages, i.e. those spanned by the g_K-V curve, both components are significant and produce bi-exponential inactivation kinetics. SqKv1A data from Sf9 cells or *Xenopus* oocytes are well described by a single exponential decay at these intermediate voltages (*data not shown*), and inactivation of the cloned channel thus does not show a multi-exponential character.

Figure 7*C* compares the steady-state voltage dependence of inactivation (measured with 1.5 sec duration prepulses; *see* inset) in a typical Sf9 cell and GFL neuron. The solid curves are fits of the Boltzmann distribution (modified to account for the nonzero current at

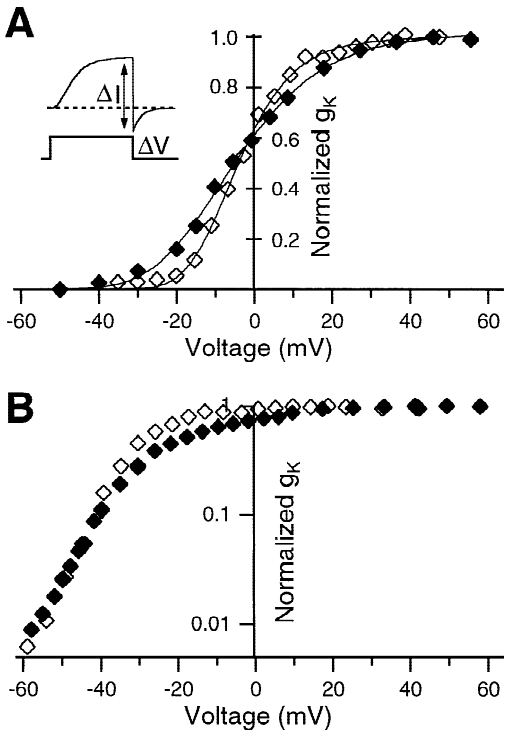

Fig. 6. Comparison of g_K-V relationships for Sf9 cells expressing SqKv1A and for GFL neurons. g_K was calculated as $\Delta I/\Delta V$ upon repolarization from the indicated voltage to −80 mV at the time of peak outward I_K (*see* inset), and values for each cell were normalized to the highest calculated value for that cell. (*A*) g_K-V relationships from a representative Sf9 cell (*open diamonds*) and a GFL cell (*closed diamonds*). The solid lines are least-squares fits of the fourth-power Boltzmann function,

$$g_K = g_{max}\left(\frac{1}{1+e^{-z(V-V_{1/2})/kT}}\right)^4,$$

where g_{max} is maximum g_K, z is the equivalent number of elementary gating charges (e_0) per subunit, V is voltage in mV, $V_{1/2}$ is the half-activation voltage in mV for a single subunit, k is Boltzmann's constant, and T is temperature (291.2°K). The illustrated functions (*solid lines*) have $V_{1/2}$ values of −19.0 mV (Sf9) *vs.* −28.5 mV (GFL) and equivalent charges (z) of 2.82 e_0 (Sf9) *vs.* 1.77 e_0 (GFL). Similar results were obtained in four cells of each type, with mean (±SEM) $V_{1/2}$ = −21.3 ± 2.5 mV (Sf9) *vs.* −29.0 ± 2.9 mV (GFL) and z = 2.7 ± 0.1 e_0 (Sf9) *vs.* 1.6 ± 0.1 e_0 (GFL). Only the difference in z is significant ($P < 0.01$) by Student's t-test. (*B*) Slope of g_K-V relationships at low relative g_K for an Sf9 cell and a GFL neuron. Sf9 data are shifted in the negative direction by 20 mV for comparison. Note that the slopes are similar (≈ e-fold/6 mV) at low relative g_K.

maximum inactivation, I_{SS}; *see* legend) with $V_{1/2}$, z, and I_{SS} values of −28.9 mV, −8.5 e_0, and 0.08 in Sf9 cells versus −26.7 mV, −5.1 e_0, and 0.31 in GFL neurons. Similar results were obtained in 4 cells of each type (*see* Fig. 7 legend). SqKv1A data from Sf9 cells has a significantly greater z value and a significantly lower level of I_{SS} ($P < 0.05$ by Student's t-test in both cases). The latter result seems consistent with the more complete inactivation of SqKv1A in Sf9 cells at positive voltages.

Effects of External TEA and K on Inactivation

Inactivation in Kv1 channels occurs through at least two distinct mechanisms. N-type inactivation is a fast process that involves the occlusion of the pore by a "ball and chain" domain of the intracellular N-terminal of an α-subunit (Hoshi, Zagotta & Aldrich, 1990; Zagotta, Hoshi & Aldrich, 1990). A more widespread and slower mechanism of inactivation called C-type involves residues near the extracellular end of the pore, in the selectivity filter, and in the S6 transmembrane helix (reviewed in Yellen, 1998). These two mechanisms can be pharmacologically distinguished in wild-type ShB channels with the impermeant blocker tetraethylammonium (TEA), which has both internal and external blocking sites (Choi, Aldrich & Yellen, 1991). N-type inactivation is slowed by internal but not external TEA, whereas C-type inactivation is slowed only by external TEA. Moreover, the degree of K channel block by TEA (fold I_K reduction) is equal to the relative increase in the inactivation time constant (fold τ_{INAC} increase), a result predicted by simple competition between TEA block and inactivation for a single open state.

External TEA reduces I_K in both SqKv1A-infected Sf9 cells and GFL neurons, but the sensitivity to TEA in the two cases is quite different with the cloned channel appearing to be ~10-fold more sensitive (Figs. 8*A* and *B*). Inactivation kinetics in Sf9 cells are substantially slowed by TEA, but this effect is not evident with GFL neurons. Fits to the traces in Fig. 8*A* and *B* give values for τ_{INAC} of 58 msec (control) *vs.* 184 msec (50 mM TEA) for the Sf9 cell and 43 msec (control) *vs.* 50 msec (500 mM TEA) for the GFL neuron. Figure 8*C* shows the relationship between the fold increase in τ_{INAC} and the fold reduction in I_K produced by a range of external TEA concentrations from experiments with both preparations. Inactivation in Sf9 cells is clearly slowed by TEA in a concentration-dependent manner, and the slope of the linear fit to these data is 0.79, a value close to 1 as predicted by the competition model. Inactivation kinetics in GFL neurons, however, are little affected by TEA, and the slope of the illustrated fit is 0.07.

C-type inactivation in a number of Kv1 channels is also slowed by high external K (Lopez-Barneo et al., 1993; Marom et al., 1993; Baukrowitz & Yellen, 1995; Rasmusson et al., 1995; Levy & Deutsch, 1996). This feature is also evident in SqKv1A-infected Sf9 cells (Fig. 9*A*), but not with the native I_K in GFL neurons (Fig. 9*B*). Results from several Sf9 cells and GFL neurons obtained over a range of K concentrations are summarized in Fig. 9*C*, which plots relative τ_{INAC} (normalized to the value in

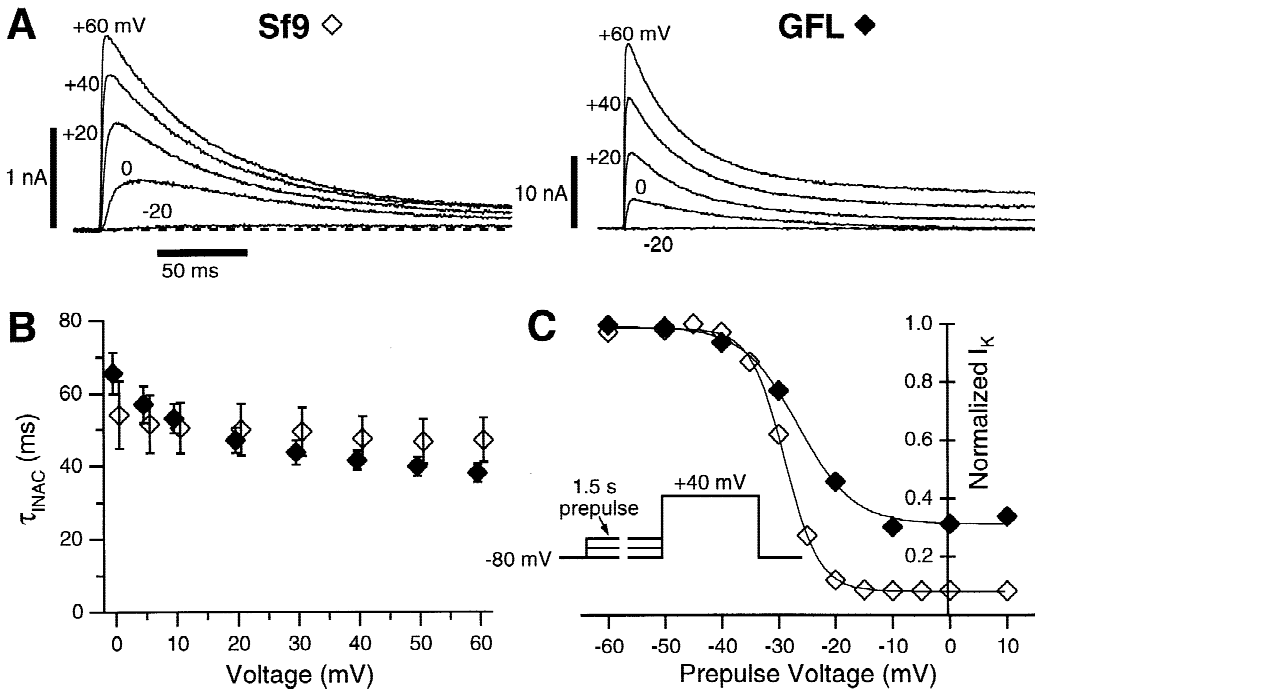

Fig. 7. Inactivation properties of I_K in Sf9 cells expressing SqKv1A and in GFL neurons. (*A*) Representative I_K families elicited with 250 msec depolarizations to the indicated voltages. (*B*) Voltage-dependence of inactivation kinetics. Time constants of inactivation (τ_{INAC}) were derived from fits of a single exponential decay function using the least squares method. Data points represent means ± SEM for 5 cells of each type. (*C*) Voltage-dependence of I_K 'steady-state' inactivation for a representative Sf9 (*open diamonds*) and GFL (*closed diamonds*) cell. Noninactivated I_K was assayed as peak I_K at +40 mV following a 1.5 sec prepulse to the indicated voltages (*see inset*). The *solid lines* are least-squares fits of a Boltzmann function modified to account for non-zero relative I_K at maximum inactivation (I_{SS}):

$$\text{relative } I_K = 1 - \frac{1 - I_{SS}}{1 + e^{-z(V - V_{1/2})/kT}}.$$

The illustrated fits have $V_{1/2}$, z, and I_{SS} values of −28.9 mV, −8.5 e_0, and 0.08 for the Sf9 cell *vs.* −26.7 mV, −5.1 e_0, and 0.31 for the GFL neuron. Similar results were obtained in 4 cells of each type with mean ± SEM fit values of: $V_{1/2} = -26.1 \pm 2.9$ mV, $z = -7.6 \pm 0.6$ e_0, $I_{SS} = 0.07 \pm 0.01$ for Sf9 cells, and $V_{1/2} = -26.3 \pm 0.1$ mV, $z = -3.9 \pm 0.6$ e_0, $I_{SS} = 0.29 \pm 0.06$ for GFL neurons. Differences in z and I_{SS} are significant ($P < 0.05$).

20 mM K) *vs.* external K concentration. The rate of inactivation depends strongly on external K in Sf9 cells but not in GFL neurons.

Discussion

Temperature-Dependent Functional Expression

Although a higher level of SqKv1A protein at 27°C *vs.* 18°C is consistent with a 27–30°C optimum for expression in Sf9 cells (Hara et al., 1992; Reuveny et al., 1993), markedly higher functional expression at 18°C has not been previously described for this system. A similar phenomenon has been reported for heterologous expression in mammalian cells, however. Temperatures below 37°C enhance surface expression of *Torpedo* acetylcholine receptors, because functional pentameric receptors are not assembled at 37°C due to misfolding of individual subunits early in biosynthesis (Claudio et al., 1987; Paulson & Claudio, 1990). Reduced temperature can also rescue functional expression of mutant CFTR channels and lutropin/chorogonadotropin receptors that do not fold properly at 37°C (Denning et al., 1992; Jaquette & Segaloff, 1997).

SqKv1A protein is naturally expressed in squid below 18°C, and low temperature might be expected to increase the fidelity of folding of this protein in Sf9 cells, either directly or through the action of specific molecular chaperones (reviewed in Hartl, 1996 and Feder & Hofmann, 1999). Alternately, low temperature could stabilize inter-subunit interactions necessary for assembly of functional channels or for ensuring long-term stability of the mature channel. Our attempts to express SqKv1A in mammalian HEK293 cells have been unsuccessful, presumably because of the even higher temperatures required.

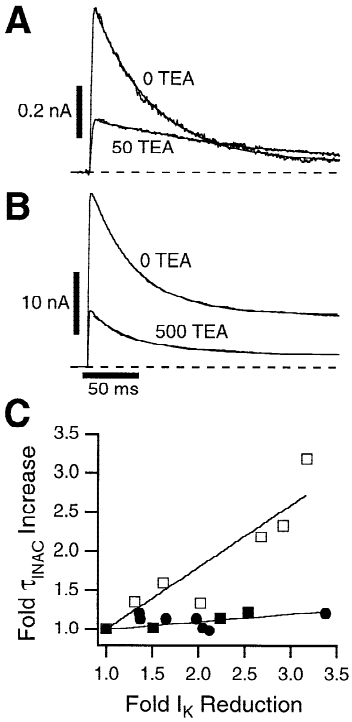

Fig. 8. Effect of external TEA on I_K inactivation in Sf9 cells expressing SqKv1A and in GFL neurons. I_K was elicited with depolarizations to +40 mV, and values of τ_{INAC} were obtained from least squares fits of a single exponential decay function. (*A*) External application of 50 mM TEA to Sf9 cells reduces peak I_K ~3-fold and slows inactivation by about the same factor. The *illustrated exponential fits* have τ_{INAC} values of 58 msec (control) and 184 msec (TEA). (*B*) 500 mM TEA is necessary to reduce GFL I_K by a similar amount, and inactivation is not markedly slowed by this concentration. The *illustrated exponential fits* have τ_{INAC} values of 43 msec (control) and 50 msec (TEA). (*C*) Relationship between I_K reduction and slowing of inactivation in Sf9 *vs.* GFL cells. Peak I_K and τ_{INAC} were measured in the absence (I_0 and τ_0) or presence of various concentrations of external TEA (I_{TEA} and τ_{TEA}) in one Sf9 cell (*open squares*) and two GFL cells (*closed squares* and *circles*). The fold-increase in τ_{INAC} at a given TEA concentration (τ_{TEA}/τ_0) was plotted against the fold-reduction in peak I_K (I_0/I_{TEA}). For Sf9 I_K, the data follow a slope of 0.79 (*solid line*). Inactivation of GFL I_K is slowed very little by external TEA, and the data are fit with a slope of 0.07 (*dotted line*). Lines were fit by the least-squares method.

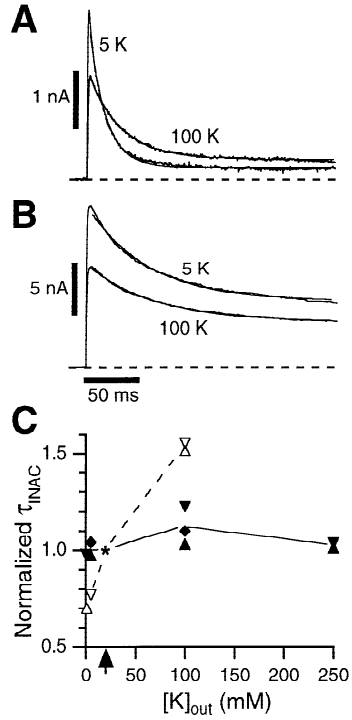

Fig. 9. Effect of external K on I_K inactivation in Sf9 cells expressing SqKv1A and in GFL neurons. I_K traces and values of τ_{INAC} were obtained as in Fig. 8. (*A*) External K slows I_K inactivation in an Sf9 cell. Values of τ_{INAC} for the *illustrated fits* were 16.1 msec (5 mM K) and 33 msec (100 mM K). (*B*) Inactivation kinetics in a GFL neuron are much less sensitive to external K. Values of τ_{INAC} for the *illustrated fits* were 58.8 msec (5 mM K) and 67 msec (100 mM K). (*C*) Dependence of τ_{INAC} on external K in two Sf9 cells (*open symbols*) and 3 GFL cells (*closed symbols*). For each cell, values of τ_{INAC} at various external K concentrations were obtained, and normalized to τ_{INAC} at 20 mM external K (τ_{20K}). τ_{20K} is thus equal to 1 by definition and is represented by an *asterisk* on the plot. Note that τ_{INAC} for Sf9 cells changes 2-fold between 0 and 100 external K, whereas values for GFL cells are stable well beyond this range.

Our finding of prolonged viability of infected cells at lower temperatures should prove useful to those wishing to extend the period during which Sf9 cells infected with other recombinant viruses are useful for physiological experiments.

Functional Differences Between Cloned and Native Channels: Activation Gating

Functional properties of GFL I_K and SqKv1A in Sf9 cells are summarized for comparison in the Table. Also included are values for SqKv1A expressed in *Xenopus* oocytes, although certain experimental parameters such as temperature and divalent ion concentrations were not identical to those of the present study (Rosenthal et al., 1996; Jerng, Liu & Gilly, 1999; Liu et al., 2001). In general, results from Sf9 cells and oocytes are similar but several specific differences are discussed below. More negative $V_{1/2}$ values from oocytes may partially reflect the low Ca concentration used (*unpublished results*).

Differences between heterologously expressed SqKv1A and GFL I_K are of interest in light of the body of evidence that associates SqKv1A with the bulk of I_K in squid giant axon system (Rosenthal et al., 1996; Rosenthal et al., 1997). Some differences, for example the exact shape of the g_K-V relation or the degree of steady-state inactivation, are fairly small, consistent with small reported differences between other cloned and native Kv1 channels (Zagotta et al., 1989; Zagotta, Hoshi &

Table 1. Selected functional properties of native squid K channels and SqKv1A homotetramers in different expression systems

	G-V (*see* Fig. 6 legend)			Activation/deactivation		
	$V_{1/2}$ (mV)	z (e_0)	Limiting slope	τ_{ON} (msec) at +40 mV	τ_{OFF} (msec) at −80 mV	τ_{OFF} slope
GFL I_K	−29.0 ± 2.9	1.6 ± 0.1	e/6 mV	0.59 ± 0.01	1.0 ± 0.2	e/54 mV
Sf9 SqKv1A	−21.5 ± 2.5	**2.7 ± 0.1**	e/6 mV	**1.03 ± 0.09**	**12.0 ± 0.7**	e/54 mV
Xenopus SqKv1A	**−41.2 ± 0.5**[a]	2.3 ± 0.2[a]	n.a.	0.72 ± 0.09[a]	**4.5 ± 0.2**[a]	e/44 mV[a]

	Inactivation kinetics				Steady-state inactivation		
	τ_{INAC} (msec) at +40 mV	Sensitive to:			$V_{1/2}$ (mV)	$z(e_0)$	I_{SS}
		V (>20 mV)	K_o	TEA_o			
GFL I_K	42 ± 3	no	no	no	−26.3 ± 0.1	−3.9 ± 0.06	0.29 ± 0.06
Sf9 SqKv1A	48 ± 6	no	**yes**	**yes**	−26.1 ± 2.9	**−7.6 ± 0.6**	**0.07 ± 0.01**
Xenopus SqKv1A	**115 ± 18**[a]	no[a]	**yes**[b]	**yes**[b]	−49.7[c]	−5.7[c]	0.02[c]

Entries in bold indicate either a qualitative difference from GLF I_K or a significant numerical difference (where SE was available) from the respective GFL I_K value ($P \leq 0.05$ by Student's t-test). Data from *Xenopus* oocytes were obtained under the following conditions. [a]Liu et al. (2001): Cell-attached patches ($N = 3$); ~21°C; external solution (mM) − 15 KCl, 127 NaCl, 6 $MgCl_2$, 1 $CaCl_2$, 5 HEPES, pH 7.1. The channel used was identical to that for Sf9 experiments except for an additional mutation (G87R) in the T1 assembly domain, which greatly increases functional expression without altering functional properties of the channel. [b]Jerng, Liu & Gilly (1999): Two-electrode configuration; ~21°C; external solution (mM) − 2 KCl, 96 NaCl, 1.8 $CaCl_2$, 2 $MgCl_2$, 5 HEPES, pH 7.0. Same channel as in [a]. [c]Rosenthal et al. (1996): Cell-attached patches; 18°C; external solution (mM) − 20 KCl, 120 NaCl, 4.5 $MgSO_4$, 5 EGTA, 5EDTA, 10 HEPES, pH 7. Same channel as in present study. N.A. = not available.

Aldrich, 1989; Grissmer et al., 1990; Pfaffinger et al., 1991) as well as between genetically identical Kv1 channels expressed in different heterologous systems (Klaiber et al., 1990). In the case of the native channel in GFL neurons, we cannot exclude the possibility that the minor presence of other K channel types (Llano et al., 1988; Nealey et al., 1993) might influence these differences. Other differences between Sf9 cells and GFL neurons such as activation and deactivation rates are more substantial, however, and cannot be ascribed to 'contamination' of the native I_K.

Although we have not yet identified the specific mechanism underlying these larger differences, even minor steric changes at residues in transmembrane helices can alter Kv1 channel gating in ways similar to that observed for native *vs.* cloned squid channels (Smith-Maxwell, Ledwell & Aldrich, 1998; Kanevsky & Aldrich, 1999). It is conceivable that such conformational perturbations could be generated by factors other than primary structure, such as post-translational modifications, association with accessory subunits, or protein-bilayer interactions. This idea is consistent with the intermediate nature of kinetics for SqKv1A channels in oocytes. In the case of SqKv1A, this hypothetical factor would influence the absolute rates at which channels undergo transitions through the activation pathway but not alter the intrinsic voltage-dependencies of these rates, which are presumably more closely tied to the primary structure of the channel protein. While glycosylation and phosphorylation are obvious candidates for such a cell-specific factor, analysis in oocytes of a number of mutations of SqKv1A in which all consensus N-linked glycosylation sites or phosphorylation (PKA and PKC) sites were eliminated has not revealed any functional effects like those discussed here (Liu, 1999; and *unpublished results*). A recently cloned squid Kvβ2 cDNA (Xu & Li, 1998) also has not revealed any effects on functional properties of SqKv1A channels in oocyte co-expression studies (*unpublished data*).

Lipid composition and cholesterol content of the plasma membrane also influence functional properties of membrane proteins (Barrantes, 1993; Gimpl et al., 1995; Klein, Gimpl & Fahrenholz, 1995; Barrantes, 1997; Gimpl, Burger & Fahrenholz, 1997), but specific effects on voltage-gated ion channel function are largely unknown. Mutations of S1, S2 or S3 residues at the putative lipid-protein interface produce effects on ShB activation gating in *Xenopus* oocytes that are very similar to those described in this report for squid channels in different cell-types (Monks, Needleman & Miller, 1999; Hong & Miller, 2000). Membranes of Sf9 cells and squid neurons have a striking difference in cholesterol content: 30% by weight in squid stellate ganglion lipids (Yamaguchi et al., 1987) *vs.* 3% in Sf9 cells maintained at 27°C under conditions employed in the present study (Gimpl et al., 1995). Membrane cholesterol content of Sf9 cells maintained at 18°C has, to the best of our knowledge, not been reported. Membrane cholesterol

levels in Sf9 cells can be manipulated through culture conditions (Gimpl et al., 1995), and this system may thus be useful in elucidating potential influences of cholesterol on K channel function.

Functional Differences Between Cloned and Native Channels: Inactivation

Rates of inactivation in 20 mM external K are virtually identical for SqKv1A in Sf9 cells and GFL I_K, but inactivation is ~2-fold slower in oocytes. This is not due to coupling to a slower activation process, and illustrates that the specific expression system can have a significant influence on inactivation gating. An intriguing qualitative difference exists in the 'pharmacology' of inactivation between native and cloned channels in both expression systems, however. External TEA and K ions slow the rate of SqKv1A inactivation in Sf9 cells as well as in *Xenopus* oocytes (Jerng et al., 1999; Table), suggesting that a conventional C-type mechanism controls inactivation (Yellen, 1998). Inactivation of I_K in GFL neurons is not slowed by external TEA or K, and an obvious question is whether an N-type mechanism is in operation. This seems unlikely, however, because slowing of inactivation by internal TEA, a characteristic of N-type inactivation, is also not observed for GFL I_K (Mathes et al., 1997).

Failure of external TEA to slow inactivation of the native channels does not necessarily preclude a C-type mechanism. The ~10-fold lower affinity of the native channel for external TEA suggests that the interaction with TEA is indeed physically disrupted in some manner, perhaps resulting in channels that can inactivate and bind TEA simultaneously. Such an alteration in the TEA binding site has been proposed for a ShBΔ point mutant in which C-type inactivation no longer competes with external TEA block (Molina, Castellano & Lopez-Barneo, 1997). Similar arguments can be made in regard to the differential effects of external K ions on inactivation in cloned and native squid channels.

Thus the mechanism of inactivation of SqKv1A and GFL I_K may not be fundamentally different. Nevertheless, the difference in TEA and K sensitivity points to a structural difference at the external end of the pore that we feel is unlikely to be due to secondary processing or membrane-channel interactions. Co-assembly of Kv1 α-subunits with other Kv1 α-subunits must therefore be seriously considered in the present context. This possibility seems the best way to reconcile the evidence for the involvement of SqKv1A in GFL I_K with the data in this report. Heteromultimers consisting of SqKv1A and a presently unknown Kv1α subunit may differ from SqKv1A homotetramers in some functional features such as the interaction with external TEA, whereas other features, such as the G-V relationship and the voltage-dependence of activation gating, may be preserved. Cooperative effects between these different subunits could also conceivably be responsible for the faster activation and deactivation kinetics of GFL I_K. While a previous attempt to identify other Kv1 transcripts was unsuccessful (Rosenthal et al., 1997), results of the current study have prompted us to revive these efforts.

We thank Dr. Min Li (Johns Hopkins School of Medicine) for the ShakerBΔ6-46 baculovirus and Dr. Rock Levinson (University of Colorado School of Medicine) for help with antibody production. This work was supported by National Institutes of Health grant NS-17510 to W.F.G., NSF predoctoral fellowship to MWB, and an NIH training grant to Stanford University.

References

Armstrong, C.M., Gilly, W.F. 1992. Access resistance and space clamp problems associated with whole-cell patch clamping. *Methods Enzymol.* **207:**100–122

Baker, O.S., Larsson, H.P., Mannuzzu, L.M., Isacoff, E.Y. 1998. Three transmembrane conformations and sequence-dependent displacement of the S4 domain in shaker K^+ channel gating. *Neuron* **20:**1283–1294

Barrantes, F.J. 1993. Structural-functional correlates of the nicotinic acetylcholine receptor and its lipid microenvironment. *FASEB J.* **7:**1460–1467

Barrantes, F.J. 1997. The acetylcholine receptor ligand-gated channel as a molecular target of disease and therapeutic agents. *Neurochem. Res.* **22:**391–400

Baukrowitz, T., Yellen, G. 1995. Modulation of K^+ current by frequency and external $[K^+]$: a tale of two inactivation mechanisms. *Neuron* **15:**951–960

Blaine, J.T., Ribera, A.B. 1998. Heteromultimeric potassium channels formed by members of the Kv2 subfamily. *J. Neurosci.* **18:**9585–9593

Brock, M.W., Gilly, W.F. 2000. Escape of an organic Kv1 blocker from enclosure in the channel cavity. *Biophys. J.* **78:**A94

Brock, M.W., Mathes, C., Gilly, W.F. 1997. SNDTT: A novel open-channel blocker of Kv1 channels. *Biophys. J.* **72:**A31

Choi, K.L., Aldrich, R.W., Yellen, G. 1991. Tetraethylammonium blockade distinguishes two inactivation mechanisms in voltage-activated K^+ channels. *Proc. Natl. Acad. Sci. USA* **88:**5092–5095

Claudio, T., Green, W.N., Hartman, D.S., Hayden, D., Paulson, H.L., Sigworth, F.J., Sine, S.M., Swedlund, A. 1987. Genetic reconstitution of functional acetylcholine receptor channels in mouse fibroblasts. *Science* **238:**1688–1694

Conti, F., Neher, E. 1980. Single channel recordings of K^+ currents in squid axons. *Nature* **285:**140–143

Denning, G.M., Anderson, M.P., Amara, J.F., Marshall, J., Smith, A.E., Welsh, M.J. 1992. Processing of mutant cystic fibrosis transmembrane conductance regulator is temperature-sensitive. *Nature* **358:**761–764

DeTomaso, A.W., Xie, Z.J., Liu, G., Mercer, R.W. 1993. Expression, targeting, and assembly of functional Na,K-ATPase polypeptides in baculovirus-infected insect cells. *J. Biol. Chem.* **268:**1470–1478

Drain, P., Dubin, A.E., Aldrich, R.W. 1994. Regulation of Shaker K^+ channel inactivation gating by the cAMP-dependent protein kinase. *Neuron* **12:**1097–1109

Dudlak, C.S., Jerng, H.H., Gilly, W.F. 2000. Tityustoxin block of native and cloned squid potassium channels is pH-dependent. *Biophys. J.* **78:**97*A.* (*Abstr.*)

Feder, M.E., Hofmann, G.E. 1999. Heat-shock proteins, molecular chaperones, and the stress response: evolutionary and ecological physiology. *Annu. Rev. Physiol.* **61:**243–282

Gilly, W.F., Lucero, M.T., Horrigan, F.T. 1990. Control of the spatial distribution of sodium channels in giant fiber lobe neurons of the squid. *Neuron* **5:**663–674

Gimpl, G., Burger, K., Fahrenholz, F. 1997. Cholesterol as modulator of receptor function. *Biochemistry* **36:**10959–10974

Gimpl, G., Klein, U., Reilander, H., Fahrenholz, F. 1995. Expression of the human oxytocin receptor in baculovirus-infected insect cells: high-affinity binding is induced by a cholesterol-cyclodextrin complex. *Biochemistry* **34:**13794–13801

Grissmer, S., Dethlefs, B., Wasmuth, J.J., Goldin, A.L., Gutman, G.A., Cahalan, M.D., Chandy, K.G. 1990. Expression and chromosomal localization of a lymphocyte K^+ channel gene. *Proc. Natl. Acad. Sci. USA* **87:**9411–9415

Hara, T., Nonaka, K., Etou, N., Ogata, S., Kawarabata, T. 1992. Escherichia coli beta-galactosidase production by baculovirus-insect cell system. *Biosci. Biotechnol. Biochem.* **56:**1124–1125

Hartl, F.U. 1996. Molecular chaperones in cellular protein folding. *Nature* **381:**571–579

Hong, K.H., Miller, C. 2000. The lipid-protein interface of a Shaker K channel. *J. Gen. Physiol.* **115:**51–58

Hoshi, T., Zagotta, W.N., Aldrich, R.W. 1990. Biophysical and molecular mechanisms of Shaker potassium channel inactivation. *Science* **250:**533–538

Isacoff, E.Y., Jan, Y.N., Jan, L.Y. 1990. Evidence for the formation of heteromultimeric potassium channels in *Xenopus* oocytes. *Nature* **345:**530–534

Jan, L.Y., Jan, Y.N. 1990. How might the diversity of potassium channels be generated? *Trends Neurosci.* **13:**415–419

Jan, L.Y., Jan, Y.N. 1997. Cloned potassium channels from eukaryotes and prokaryotes. *Annu. Rev. Neurosci.* **20:**91–123

Jaquette, J., Segaloff, D.L. 1997. Temperature sensitivity of some mutants of the lutropin/choriogonadotropin receptor. *Endocrinology* **138:**85–91

Jerng, H.H., Gilly, W.F. 2000. Changes in unitary conductance underlie MgATP-modulation of inactivation in squid K channels. *Biophys. J.* **78:***A*208 (*Abstr.*)

Jerng, H.H., Liu, T., Gilly, W.F. 1999. C-type inactivation of a cloned squid K^+ channel expressed in *Xenopus* oocytes. *Biophys. J.* **76:**A191 (*Abstr.*)

Kanevsky, M., Aldrich, R.W. 1999. Determinants of voltage-dependent gating and open-state stability in the S5 segment of Shaker potassium channels. *J. Gen. Physiol.* **114:**215–242

Klaiber, K., Williams, N., Roberts, T.M., Papazian, D.M., Jan, L.Y., Miller, C. 1990. Functional expression of Shaker K^+ channels in a baculovirus-infected insect cell line. *Neuron* **5:**221–226

Klein, U., Gimpl, G., Fahrenholz, F. 1995. Alteration of the myometrial plasma membrane cholesterol content with beta-cyclodextrin modulates the binding affinity of the oxytocin receptor. *Biochemistry* **34:**13784–13793

Levitan, I.B. 1994. Modulation of ion channels by protein phosphorylation and dephosphorylation. *Annu. Rev. Physiol.* **56:**193–212

Levy, D.I., Deutsch, C. 1996. Recovery from C-type inactivation is modulated by extracellular potassium. *Biophys. J.* **70:**798–805

Liu, T. 1999. A family of squid Kv1 potassium channels: localization in squid nervous system and regulation of heterologous expression in *Xenopus* oocytes. Stanford University, Stanford, CA

Liu, T.I., Lebaric, Z.N., Rosenthal, J.J.C., Gilly, W.F. 2001. Natural substitutions at highly conserved T1-domain residues perturb processing and functional expression of squid Kv1 channels. *J. Neurophysiol.* **85:**61–71

Llano, I., Bookman, R.J. 1986. Ionic conductances of squid giant fiber lobe neurons. *J. Gen. Physiol.* **88:**543–569

Llano, I., Webb, C.K., Bezanilla, F. 1988. Potassium conductance of the squid giant axon. Single-channel studies. *J. Gen. Physiol.* **92:**179–196

Lopez-Barneo, J., Hoshi, T., Heinemann, S.H., Aldrich, R.W. 1993. Effects of external cations and mutations in the pore region on C-type inactivation of Shaker potassium channels. *Receptors Channels* **1:**61–71

Marom, S., Goldstein, S.A., Kupper, J., Levitan, I.B. 1993. Mechanism and modulation of inactivation of the Kv3 potassium channel. *Receptors Channels* **1:**81–88

Mathes, C., Rosenthal, J.J., Armstrong, G.M., Gilly, W.F. 1997. Fast inactivation of delayed rectifier K conductance in squid giant axon and its cell bodies. *J. Gen. Physiol.* **109:**435–448

McCormack, K., Lin, J.W., Iverson, L.E., Rudy, B. 1990. Shaker K^+ channel subunits from heteromultimeric channels with novel functional properties. *Biochem. Biophys. Res. Commun.* **171:**1361–1371

Molina, A., Castellano, A.G., Lopez-Barneo, J. 1997. Pore mutations in Shaker K^+ channels distinguish between the sites of tetraethylammonium blockade and C-type inactivation. *J. Physiol.* **499:**361–367

Monks, S.A., Needleman, D.J., Miller, C. 1999. Helical structure and packing orientation of the S2 segment in the Shaker K^+ channel. *J. Gen. Physiol.* **113:**415–423

Nealey, T., Spires, S., Eatock, R.A., Begenisich, T. 1993. Potassium channels in squid neuron cell bodies: comparison to axonal channels. *J. Membrane Biol.* **132:**13–25

Paulson, H.L., Claudio, T. 1990. Temperature-sensitive expression of all-Torpedo and Torpedo-rat hybrid AChR in mammalian muscle cells. *J. Cell Biol.* **110:**1705–1717

Perozo, E., Jong, D.S., Bezanilla, F. 1991. Single channel studies of the phosphorylation of K^+ channels in the squid giant axon. II. Nonstationary conditions. *J. Gen. Physiol.* **98:**19–34

Perozo, E., Vandenberg, C.A., Jong, D.S., Bezanilla, F. 1991. Single channel studies of the phosphorylation of K^+ channels in the squid giant axon. I. Steady-state conditions. *J. Gen. Physiol.* **98:**1–17

Pfaffinger, P.J., Furukawa, Y., Zhao, B., Dugan, D., Kandel, E.R. 1991. Cloning and expression of an Aplysia K^+ channel and comparison with native Aplysia K^+ currents. *J. Neurosci.* **11:**918–927

Pongs, O., Leicher, T., Berger, M., Roeper, J., Bähring, R., Wray, D., Giese, K.P., Silva, A.J., Storm, J.F. 1999. Functional and molecular aspects of voltage-gated K^+ channel beta subunits. *Ann. N. Y. Acad. Sci.* **868:**344–355

Rasmusson, R.L., Morales, M.J., Castellino, R.C., Zhang, Y., Campbell, D.L., Strauss, H.C. 1995. C-type inactivation controls recovery in a fast inactivating cardiac K^+ channel (Kv1.4) expressed in *Xenopus* oocytes. *J. Physiol.* **489:**709–721

Reuveny, S., Kim, Y.J., Kemp, C.W., Shiloach, J. 1993. Effect of temperature and oxygen on cell growth and recombinant protein production in insect cell cultures. *Appl. Microbiol. Biotechnol.* **38:**619–623

Rosenthal, J.J., Liu, T.I., Gilly, W.F. 1997. A family of delayed rectifier Kv1 cDNAs showing cell type-specific expression in the squid stellate ganglion/giant fiber lobe complex. *J. Neurosci.* **17:**5070–5079

Rosenthal, J.J., Vickery, R.G., Gilly, W.F. 1996. Molecular identification of SqKv1A. A candidate for the delayed rectifier K channel in squid giant axon. *J. Gen. Physiol.* **108:**207–219

Rudy, B. 1988. Diversity and ubiquity of K channels. *Neuroscience* **25:**729–749

Ruppersberg, J.P., Schroter, K.H., Sakmann, B., Stocker, M., Sewing, S., Pongs, O. 1990. Heteromultimeric channels formed by rat brain potassium-channel proteins. *Nature* **345:**535–537

Santacruz-Toloza, L., Huang, Y., John, S.A., Papazian, D.M. 1994.

Glycosylation of shaker potassium channel protein in insect cell culture and in *Xenopus* oocytes. *Biochemistry* **33:**5607–5613

Schoppa, N.E., Sigworth, F.J. 1998*a*. Activation of shaker potassium channels. I. Characterization of voltage-dependent transitions. *J. Gen. Physiol.* **111:**271–294

Schoppa, N.E., Sigworth, F.J. 1998*b*. Activation of shaker potassium channels. III. An activation gating model for wild-type and V2 mutant channels. *J. Gen. Physiol.* **111:**313–342

Schulteis, C.T., Nagaya, N., Papazian, D.M. 1996. Intersubunit interaction between amino- and carboxyl-terminal cysteine residues in tetrameric shaker K^+ channels. *Biochemistry* **35:**12133–12140

Shen, N.V., Chen, X., Boyer, M.M., Pfaffinger, P.J. 1993. Deletion analysis of K^+ channel assembly. *Neuron* **11:**67–76

Sheng, M., Liao, Y.J., Jan, Y.N., Jan, L.Y. 1993. Presynaptic A-current based on heteromultimeric K^+ channels detected in vivo. *Nature* **365:**72–75

Smith-Maxwell, C.J., Ledwell, J.L., Aldrich, R.W. 1998. Uncharged S4 residues and cooperativity in voltage-dependent potassium channel activation. *J. Gen. Physiol.* **111:**421–439

Summers, M.D., Smith, G.E. 1987. A manual of methods for baculovirus vectors and insect cell culture procedures. Texas Agricultural Experiment Station, College Station, TX

Thornhill, W.B., Wu, M.B., Jiang, X., Wu, X., Morgan, P.T., Margiotta, J.F. 1996. Expression of Kv1.1 delayed rectifier potassium channels in Lec mutant Chinese hamster ovary cell lines reveals a role for sialidation in channel function. *J. Biol. Chem.* **271:**19093–19098

Wang, H., Kunkel, D.D., Martin, T.M., Schwartzkroin, P.A., Tempel, B.L. 1993. Heteromultimeric K^+ channels in terminal and juxtaparanodal regions of neurons. *Nature* **365:**75–79

Weiser, M., Vega-Saenz de Miera, E., Kentros, C., Moreno, H., Franzen, L., Hillman, D., Baker, H., Rudy, B. 1994. Differential expression of Shaw-related K^+ channels in the rat central nervous system. *J. Neurosci.* **14:**949–972

Xu, J., Li, M. 1998. Auxilliary subunits of Shaker-type potassium channels. *Trends. Cardiovas. Med.* **8:**229–234

Yamaguchi, H., Tanaka, T., Ichioka, T., Stoskopf, M., Kishimoto, Y., Gould, R. 1987. Characterization and comparison of lipids in different squid nervous tissues. *Biochim. Biophys. Acta* **922:**78–84

Yellen, G. 1998. The moving parts of voltage-gated ion channels. *Quart. Rev. Biophys.* **31:**239–295

Yu, W., Xu, J., Li, M. 1996. NAB domain is essential for the subunit assembly of both alpha-alpha and alpha-beta complexes of shaker-like potassium channels. *Neuron* **16:**441–453

Zagotta, W.N., Germeraad, S., Garber, S.S., Hoshi, T., Aldrich, R.W. 1989*a*. Properties of ShB A-type potassium channels expressed in Shaker mutant Drosophila by germline transformation. *Neuron* **3:**773–782

Zagotta, W.N., Hoshi, T., Aldrich, R.W. 1989*b*. Gating of single Shaker potassium channels in Drosophila muscle and in *Xenopus* oocytes injected with Shaker mRNA. *Proc. Natl. Acad. Sci. USA* **86:**7243–7247

Zagotta, W.N., Hoshi, T., Aldrich, R.W. 1990. Restoration of inactivation in mutants of Shaker potassium channels by a peptide derived from ShB. *Science* **250:**568–571

Zagotta, W.N., Hoshi, T., Aldrich, R.W. 1994. Shaker potassium channel gating. III: Evaluation of kinetic models for activation. *J. Gen. Physiol.* **103:**321–362

Zagotta, W.N., Hoshi, T., Dittman, J., Aldrich, R.W. 1994. Shaker potassium channel gating. II: Transitions in the activation pathway. *J. Gen. Physiol.* **103:**279–319